

# Influence of Dense Non-Aqueous Phase Liquids Properties and Geotechnical Conditions on the Migration Processes in Sandy Media

Masashi KAMON, Kazuto ENDO\*, Takeshi KATSUMI\*\*

\* Graduate School of Engineering, Kyoto University

\*\* Department of Civil Engineering, Ritsumeikan University

## Synopsis

Migration properties of dense non-aqueous phase liquids (DNAPLs) in the subsurface can be expressed as a water-NAPL two-phase system based on the permeability ( $k$ ), saturation ( $S$ ), and pressure ( $p$ ), similar to an unsaturated water-air two-phase system. This relation is called “ $k$ - $S$ - $p$  relation”. In this paper, first, the concept of the migration processes under the liquid-liquid immiscible two-phase flow condition is presented. Second, to estimate the influence of the fluid properties and subsurface conditions on the  $k$ - $S$ - $p$  relations, the analysis for these parameters is performed by using the finite element code MOFAT. Finally, two-dimensional tank analyses in homogenous and heterogeneous subsurface conditions are performed for evaluating the effect of the rate of groundwater flow. This numerical results indicate the fundamental behavior of DNAPL migration under the two-phase flow system in the aquifer.

**Keywords:** Dence non-aqueous phase liquids,  $k$ - $S$ - $p$  relations, fluid properties, subsurface conditions, groundwater

## 1. Introduction

Soil and groundwater contamination with non-aqueous phase liquids (NAPLs), such as volatile organic compounds (VOCs), have received increasing attention in the last decade. NAPLs can be classified into DNAPLs (Dense-NAPLs) and LNAPLs (Light-NAPLs). DNAPLs, such as Trichloroethane (TCE) and Perchloroethylene (PCE), are the liquids with specific gravities larger than water, and in general, have little solubility to water. Thus, they can exist and migrate in soil/porous pores as independent phases. A typical DNAPL migration in a homogenous and heterogeneous condition in the subsurface is shown in Fig. 1. In homogenous condition, the DNAPL plume in the subsurface migrates only downward without having influence on the groundwater lateral flow, and then

it may form a contaminated column due to its larger density. Subsequently, small amount of dissolved substances gradually diffuses in groundwater from the column formed by DNAPL. Residual DNAPL phase also becomes a source of the diffusion. DNAPL plume often accumulates at the bottom of the subsurface, and this accumulated plume is called DNAPL pool. The region, which contains higher degree of DNAPL saturation than the residual DNAPL saturation, is also called DNAPL pool at any location in the subsurface. In heterogeneous condition, the DNAPL plume migrates downward until it encounters an impermeable layer (e.g., clayey soil layer/lens), and then the direction of DNAPL migration alters from vertical to horizontal flow. The horizontal DNAPL migration continues until DNAPL pressure increases to be able to penetrate through the clayey layer/lens, or until DNAPL

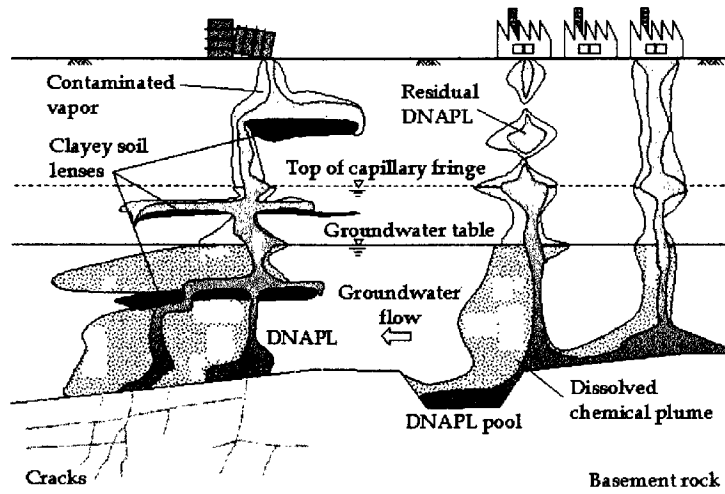


Fig. 1 Typical DNAPL migration processes in the subsurface

source encounters a permeable layer. If the basement rock has some cracks, then DNAPL plume invades into the cracks.

Attempts have been made to treat contaminated soil and groundwater by the pump-and-treat method, bioremediation, surfactants/cosolvents method, and permeable reactive barrier. In order to verify the efficiency of these remediation methods, to develop the remediation techniques, and to characterize the contaminated sites, it is necessary to know properly the DNAPL migration process. Therefore, the aim of this paper is to obtain and clarify the fundamental concept for DNAPL migration under the immiscible two-phase flow condition. In this paper, DNAPL is assumed to be an inert solvent (i.e., involatile, insoluble one), thus, the solute transport model is not considered.

## 2. Conceptual Modeling

### 2.1 Governing equation

Fluid flow in porous media is generally treated as a steady laminar flow, that is, the speed of the fluid flow is lower than the threshold for turbulent flow. The equation describing the fluid flow in porous media, called Darcy's law, generalized for multiphase flow is given by

$$q_{\alpha i} = -\frac{k_{r\alpha}K}{\mu_{\alpha}}(\nabla P_{\alpha} + \rho_{\alpha}g\nabla z) \quad (1)$$

where  $q_{\alpha i}$  is the fluid flux or so-called Darcy velocity of  $\alpha$  phase in the  $i$  direction,  $k_{r\alpha}$  the relative permeability of  $\alpha$  phase,  $K$  the intrinsic permeability tensor of the porous media,  $\mu_{\alpha}$  the viscosity of  $\alpha$  phase,  $P_{\alpha}$  the

liquid pressure of  $\alpha$  phase,  $g$  the gravitational acceleration, and  $z$  the elevation head. Phase  $\alpha$  stands for either air(A), wetting phase(W), or nonwetting phase(NW). In environmental geotechnical field, instead of working with the concept of a liquid pressure  $P_{\alpha}$ , the concept of a water-equivalent/liquid-pressure head  $h_{\alpha}$  is used:

$$h_{\alpha} = \frac{P_{\alpha}}{\rho_w g} \quad (2)$$

where  $\rho_w$  designates the density of water. Thus, the Darcy's law expressed by the concept of water-equivalent head becomes

$$q_{\alpha i} = -\frac{k_{r\alpha}K}{\mu_{\alpha}}\rho_w g(\nabla h_{\alpha} - \rho_{r\alpha}\nabla z) \quad (3)$$

where  $\rho_{r\alpha} = \rho_{\alpha}/\rho_w$ ,  $\rho_{r\alpha}$  is the relative density of  $\alpha$  phase.

The continuity equation for an incompressible porous media is given by

$$\Phi \frac{\partial t}{\partial S_{\alpha}} = -\nabla \cdot (\rho_{\alpha}q_{\alpha i}) + Q_{\alpha} \quad (4)$$

where  $\Phi$  is the porosity of the porous medium,  $S_{\alpha}$  the degree of  $\alpha$  phase saturation, and  $Q_{\alpha}$  the source-sink term due to the transfer of mass between phases. Assuming that the density is a constant within the  $\alpha$  phase, and there is no source-sink term, the governing equation for multiphase flow through a porous media is obtained by substituting Eqn.(3) into Eqn.(4) (Parker, 1989)

$$\Phi \frac{\partial S_{\alpha}}{\partial t} - \nabla \cdot \left( \frac{k_{r\alpha}K}{\mu_{\alpha}}\rho_w g(\nabla h_{\alpha} - \rho_{r\alpha}\nabla z) \right) \quad (5)$$

In this governing equation for multiphase flow, unlike the porosity, the density, the viscosity, and the intrinsic

permeability, which are usually assumed to be time independent parameters, the degree of saturation, the relative permeability, and pressure head all vary according to the elapsed time, and yield so-called  $k$ - $S$ - $p$  relations (Parker and Lenhard, 1987; Lenhard and Parker, 1987b). Hence, in order to solve the equation, that is, to solve the contamination problems, the intrinsic permeability and the  $k$ - $S$ - $p$  relations should be clarified.

## 2.2 Capillary pressure head

Capillary pressure of pore-fluid systems is an important parameter in the research of the behavior of porous media containing two/more immiscible fluid systems, such as air-water, oil-water, and air-NAPL-water systems. Capillary pressure  $P_c$  is defined as

$$P_c \equiv P_{NW} - P_W \quad (6)$$

where  $P_{NW}$  is liquid pressure in the non-wetting phase (e.g., air, oil, and NAPL phases),  $P_W$  the liquid pressure in the wetting phase (water). The capillary pressure can also be defined as the pressure difference between immiscible two phases across the interface dividing into two phases. The capillary pressure depends on the interfacial/surface tension, the contact angle, and the radii of the fluid curvature in capillaries formed by soil particles.

In water-air two-phase system, namely under the unsaturated condition, the capillary pressure is given by

$$P_c = P_a - P_W \quad (7)$$

where  $P_a$  is pore air pressure. In general, laboratory experiment is performed under the atmospheric pressure, thus the pore air pressure also may be taken as the atmospheric pressure. A standard/hydrophilic tensiometer can measure the negative pore water pressure taking the reference pressure as the atmospheric pressure. Therefore, the reading of pressure gauge from the tensiometer directly indicates the negative pore water pressure, so-called matric potential and capillary pressure head.

In the case of water and NAPL system, it needs two kinds of tensiometers to measure the capillary pressure, because the capillary pressure is calculated by the pressure difference between pore water pressure and pore DNAPL pressure. One of them is a hydrophilic tensiometer in order to measure the pore water pressure in porous media, and another one is a hydrophobic tensiometer to measure the pore DNAPL pressure. Therefore, the capillary pressure can be cal-

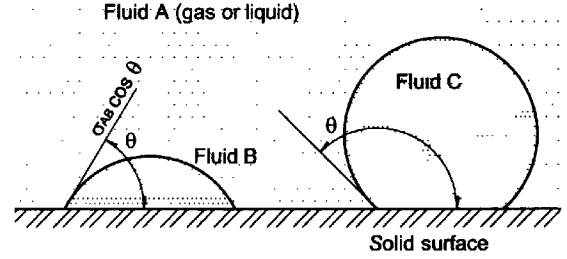


Fig. 2 Liquid shape on a solid surface

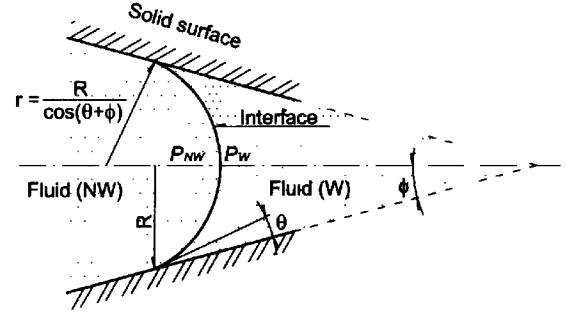


Fig. 3 Meniscus in a conical capillary

culated simply as the pressure difference between the larger value and smaller one (Dullien, 1992).

Among the many parameters having an influence on the migration process, wettability may be the representative one. The wettability represents the affinity of one immiscible fluid for a solid surface in the presence of one more immiscible fluid. Figure 2 shows two immiscible liquids (or a liquid and a gas) contact with a solid surface. The contact angle  $\theta$  denotes the angle between the interface of these fluids and the solid surface, and the product  $\sigma_{AB} \cos \theta$  is called the adhesion tension, where  $\sigma$  is the interfacial/surface tension between fluid A and B. When  $\theta < 90^\circ$ , the fluid B is called the wetting fluid (phase). When  $\theta > 90^\circ$ , the fluid C is called a nonwetting fluid (phase) (Bear, 1972).

Figure 3 shows the meniscus in a conical capillary (Dullien, 1992). The capillary pressure  $P_c$  defined as the pressure difference between  $P_W$  and  $P_{NW}$  in this figure is given by

$$P_c = P_{NW} - P_W = (2\sigma/R) |\cos(\theta + \phi)| \quad (8)$$

in which

$$r = \frac{R}{\cos(\theta + \phi)} \quad (9)$$

where  $\theta$  is the contact angle,  $\phi$  is the angle of the tilted orientation, that is, the angle of the conical pore space,

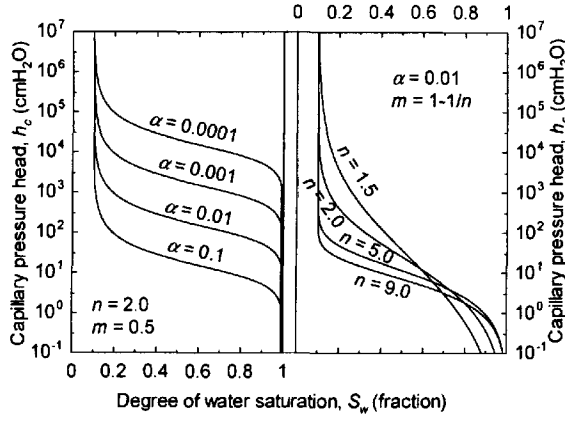


**Fig. 4** Influence of the VG parameter  $\alpha$  and  $n$  on the  $S-p$  relations

$r$  is the mean radius of the curvature. If the solid surface is parallel (i.e., tilted angle is 0) and the contact angle is 0, then  $P_c$  is defined as  $2\sigma/r$  (Perloff and Baron, 1976).

### 2.3 $k-S-p$ relations

The relation between the degree of water saturation,  $S_w$ , and the capillary pressure head,  $h_c$ , of the unsaturated porous media (i.e., water-air system) with immiscible two-phase fluids, pair  $i$  and  $j$ , is referred to as a water retention curve or  $S-p$  relations, where  $i$  and  $j$  stand for air(A), water(W), and nonwetting fluid(NW). The empirical parametric form, called the VG model, is given by van Genuchten (1980), and the equation solved for  $h_c$  may be written as (Helmig, 1997)

$$h_c = \frac{1}{\alpha} \left( S_{je}^{-1/m} - 1 \right)^{1/n} ; \quad \text{for } h_c > 0 \quad (10)$$

where  $\alpha$  and  $n$  are the VG parameters, and  $m = 1 - 1/n$ , and where the effective saturation of the  $j$  phase,  $S_{je}$ , is defined as

$$S_{je} = \frac{S_j - S_{jr}}{1 - S_{jr}} \quad (11)$$

with  $S_{jr}$  being the residual or the irreducible saturation. Figure 4 shows the influence of the VG parameters,  $\alpha$  and  $n$ , on the water retention curves. The curve shifts upward as  $\alpha$  decreases. The parameter  $n$  indicates the gradient of the curves. In this case of a soil with low uniformity coefficient,  $n$  takes a large value.

Another empirical form of the water retention curve, called the BC model, was given by Brooks and Corey (1964), and the equation solved for  $h_c$  is written as

$$h_c = h_d S_{je}^{-1/\lambda} ; \quad \text{for } h_c \geq h_d \quad (12)$$

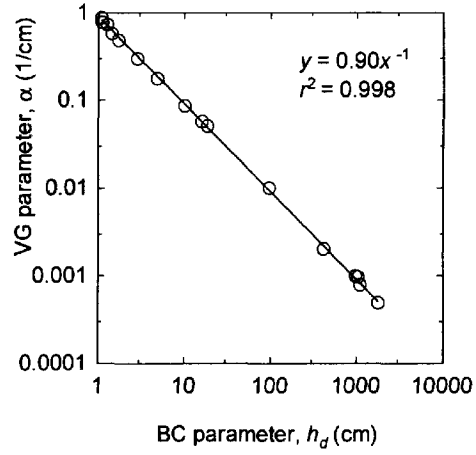


**Fig. 5** The relationship between the BC parameter  $h_d$  and the VG parameter  $\alpha$

where  $\lambda$  indicates the pore distribution index and  $h_d$  is the displacement head of the reference two phases system, that is, the displacement pressure head from the phase  $j$  to another phase  $i$ . The VG parameter  $\alpha$  has a similar meaning of the displacement pressure head  $h_d$  on the BC model. These relationships, which were obtained by both the VG and the BC fittings for hypothetical values, are shown in Fig. 5. It is found that the approximated equation has a strong correlation.

The method for predicting relative permeability  $k_{ri}$  is also proposed as the VG and the BC models, and the value of the relative permeability is estimated from the parameters of the  $S-p$  relations. The relative permeability usually ranges from 0 to 1, and it reaches 1 when the porous media is saturated with the reference phase  $i$ . The relative permeability of water,  $k_{rW}$ , and the DNAPL phase,  $k_{rNW}$ , are given by the following equations;

$$k_{rW} = S_e^\epsilon \left[ 1 - \left( 1 - S_e^{(1/m)} \right)^m \right]^2 \quad (13)$$

$$k_{rNW} = (1 - S_e)^\gamma \left[ 1 - S_e^{(1/m)} \right]^{2m} \quad (14)$$

where  $\epsilon$  and  $\gamma$  representing the conductivity of pore structure take  $\epsilon = 1/2$  and  $\gamma = 1/3$  (Helmig, 1997), while the BC model,

$$k_{rW} = S_e^{\left( \frac{2+\lambda}{\lambda} \right)} \quad (15)$$

$$k_{rNW} = (1 - S_e)^2 \left( 1 - S_e^{\left( \frac{2+\lambda}{\lambda} \right)} \right) \quad (16)$$

### 2.4 Scaling factor

The difference between the  $S-p$  curves of the water-air and the water-oil/DNAPL system may be

**Table 1** Properties of the DNAPL substitutes and the representative VOCs (20 °C)

Terms		HFE-7100	PF-5080	TCE	PCE	Water
Chemical formula	—	C <sub>4</sub> F <sub>9</sub> OCH <sub>3</sub>	C <sub>8</sub> F <sub>18</sub>	C <sub>2</sub> HCl <sub>3</sub>	C <sub>2</sub> Cl <sub>4</sub>	H <sub>2</sub> O
Specific gravity	—	1.52	1.76	1.464	1.623	0.998
Relative viscosity	—	0.58	1.23	0.59	0.90	1.00
Surface tension	mN/m	13.6	15	29.30	31.30	72.75
Interfacial tension	mN/m	—	—	34.50	44.40	none
Vapor pressure	kPa	28	3.87	7.73	2.13	2.34
Solubility in water	ppm	12	11	110	15	none

scaled by introducing a scaling factor  $\beta_{ij}$  (Lenhard and Parker, 1987a). The scaling factor is defined as

$$\beta_{ij} = \frac{\sigma^*}{\sigma_{ij}} \quad (17)$$

where  $\sigma^*$  is the interfacial tension of the reference fluid pair, and  $\sigma_{ij}$  is the interfacial tension between fluids  $i$  and  $j$ . Choosing a reference system is arbitrary, but a natural choice would be the surface tension of the water-air fluid pair. Thus the scaled VG model can be expressed as

$$S^* = [1 + (\alpha \cdot h^*)^n]^{-m} \quad (18)$$

where  $S^* = S_{ej}$  and  $h^* = \beta_{ij} h_{ij}$ . Applying the same scaling procedure to the BC model,

$$S^* = \left( \frac{h_d}{h^*} \right) \quad (19)$$

can be obtained.

### 3. One-dimensional Modeling

One-dimensional vertical column model is analyzed in order to clarify the fundamental concept of DNAPL migration processes. Vertical column test is also performed experimentally with new probes for measuring the degree of water saturation and pore liquids pressure. The apparatus used to measure the migration properties of an immiscible two-phase flow is illustrated in Fig. 6 (Kamon et al., 2001). The column has 3.5 cm in inside diameter and 50 cm long in length. Toyoura sand with a soil particle density of 2.64 g/cm<sup>3</sup> is used as a porous media, and the sand porous media is prepared with porosity of 0.38. Three hydrophilic and three hydrophobic tensiometers for measuring pore water and pore DNAPL pressure, respectively, as well as five three-electrode electrical conductivity probes for measuring the degree of water saturation are inserted into the specimen from the side of the column. As substitutes for DNAPLs, Hydrofluoroether, HFE-7100, and Performance Fluid, PF-5080,

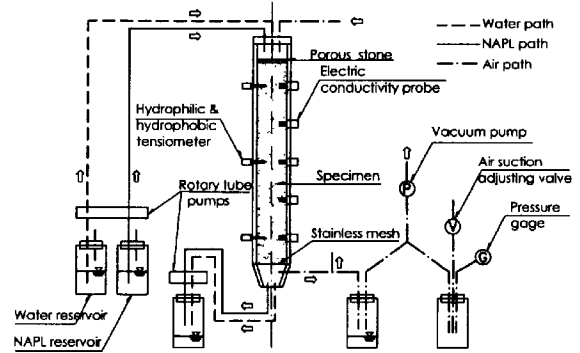


**Fig. 6** The apparatus for multiphase column test

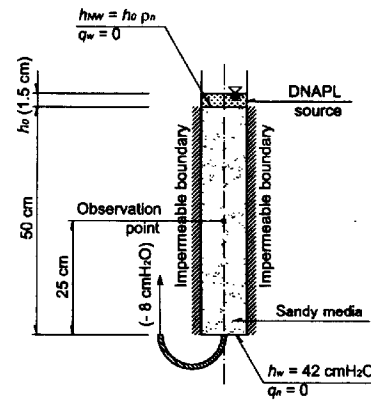


**Fig. 7** The boundary condition of the one-dimensional vertical column model

(both liquids produced by 3M<sup>TM</sup>) are used for the sake of safety. The properties of these fluids and the representative VOCs are summarized in Table 1.

### 3.1 Numerical approach

In order to make clear the concept of DNAPL migration process below the groundwater table, numerical analyses are performed by using two-dimensional finite element code MOFAT (Kaluarachchi and Parker, 1989). The analyzed parameters are described as fol-

**Table 2** The analytical parameter for the column model simulation

Cases	Fluid properties				Geotechnical constants		VG parameters	
	relative density –	relative viscosity –	$\beta_{NW}$ –	interfacial tension mN/m	hydraulic conductivity cm/s	porosity –	$\alpha$ 1/cm	$n$ –
Head	1.50	0.50	1.50	48.5	$10^{-3}$	0.35	0.100	5.00
Density	1.10 - 1.90	0.50	1.50	48.5	$10^{-3}$	0.35	0.100	5.00
Viscosity	1.50	0.10 - 1.50	1.50	48.5	$10^{-3}$	0.35	0.100	5.00
$\beta_{NW}$	1.50	0.50	1.10 - 3.50	20.8 - 66.1	$10^{-3}$	0.35	0.100	5.00
Hydraulic conductivity	1.50	0.50	1.50	48.5	$10^{-2}$ - $10^{-6}$	0.35	0.100	5.00
porosity	1.50	0.50	1.50	48.5	$10^{-3}$	0.65	0.100	5.00
						0.30 - 0.65	0.100	5.00

lows and tabulated in Table 2; (1) the influence of the pressure head as the boundary condition, (2) the influence of the fluid properties such as the fluid density, viscosity, and interfacial tension (i.e., scaling factor  $\beta$ ), (3) the influence of the porosity and the hydraulic conductivity as geotechnical constants. In these analyses, DNAPL is assumed to be an inert solvent, and the standard conditions are fixed such that the hydraulic conductivity is  $10^{-3}$  cm/s, the porosity 0.35, the VG parameter  $\alpha = 0.10$ ,  $n = 5.00$ , the residual water saturation  $S_{rw}$  0.15, the residual DNAPL saturation  $S_{rNW}$  0.20, DNAPL density is  $1.50 \text{ g/cm}^3$ , the relative viscosity of DNAPL is 0.50, and the interfacial tension  $48.5 \text{ mN/m}$ , that is,  $\beta_{ij} = 1.50$ . As an initial state, the physical system of a 50-cm-long column with sandy media under the water-saturated condition is taken. The boundary conditions for this analysis are shown in Fig. 7. The analysis in each case was terminated when the DNAPL phase reached to the bottom of the column, where the observation point is set at 25 cm upward from the bottom (i.e., at the center of the column). The migration process is evaluated for a variety of the degree of DNAPL saturation  $S_{NW}$  against the elapsed time.

### (1) The boundary condition

In Fig. 7, the height of DNAPL source,  $h_0$ , is applied as a variable external pressure head, and the influence of  $h_0$  on the migration process is evaluated. The height of DNAPL source  $h_0$  ranges from 1 cm to 10 cm, that is, the actual applied water-equivalent head ranges from  $1.5 \text{ cmH}_2\text{O}$  to  $15 \text{ cmH}_2\text{O}$ , because the hypothetical fluid density is  $1.5 \text{ g/cm}^3$ . The change in the degree of DNAPL saturation against the elapsed time at the observation point is shown in Fig. 8. Increase in  $h_0$  results in the shortage of time in which the NAPL reaches the observation point. The maximum degree of DNAPL saturation also increases with increasing  $h_0$ .

From this figure, it is found that the migration rate as well as the maximum degree of DNAPL saturation depends on the applied head.

### (2) Fluid properties

The influence of the DNAPL density on the DNAPL migration is shown in Fig. 9. This analysis is performed under the condition that the relative viscosity is taken as a constant, 0.50. The arrived time at the observation point becomes shorter with increasing density, and the maximum DNAPL saturation decreases as the density increases. Figure 10 shows the influence of the DNAPL viscosity on the migration. Both the breakthrough time and the maximum DNAPL saturation increase with increasing DNAPL viscosity. It is interesting to note that the migration rate varies exponentially with the density, while it varies linearly with the viscosity of DNAPL. Figure 11 shows the influence of the interfacial tension between water and DNAPL, that is, the influence of the scaling factor  $\beta_{NW}$ . The  $\beta$  does not affect the breakthrough time at the observation point, but the maximum DNAPL saturation is affected by  $\beta$ , and then it increases with increasing  $\beta$  (i.e., decreasing the interfacial tension). The saturation also varies exponentially in a similar tendency as in the influence of the fluid density. From these results, in this condition, it is inferred that the contamination by the DNAPL with low viscosity, low interfacial tension, and high density makes rapid progress. Furthermore, induces the most serious problem after a long time, because the amount of this DNAPL becomes large.

### (3) Subsurface conditions

In order to investigate the influence of the subsurface conditions, such as the hydraulic conductivity and the porosity, on the DNAPL migration process, the numerical simulation is performed. The arrived time increasing linearly with decreasing hydraulic con-

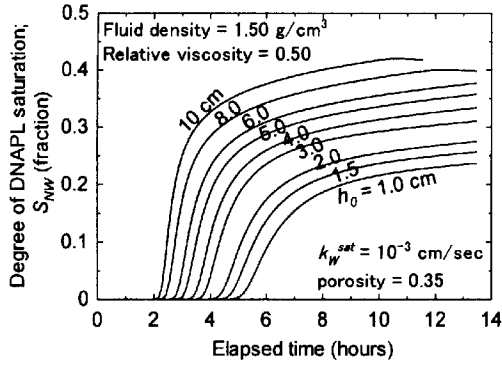


**Fig. 8** Influence of the external pressure head on the migration process

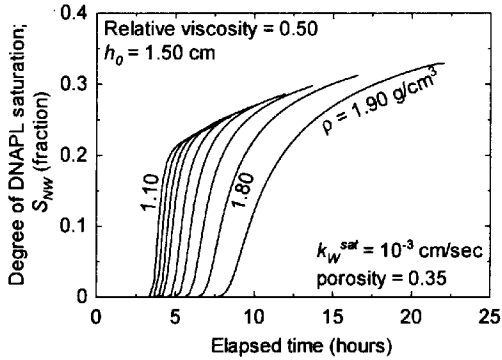


**Fig. 9** Influence of the DNAPL density on the migration process

ductivity, and the changing process in the degree of DNAPL saturation against the elapsed time take the same shape for both all hydraulic conductivity and all porosity cases. The arrived time, when the porosity of the medium is 0.35, becomes shorter than the case of larger porosity 0.65. This reason is that the real velocity  $v_i$  defined by (Kinzelbach, 1986)

$$v_i = \frac{q\alpha_i}{\Phi} \quad (20)$$

in the pore of a porous system increases with decreasing porosity under the constant hydraulic gradient caused by the fixed boundary condition.

In the case that the porous media has different porosity with equal hydraulic conductivity  $10^{-3}$  cm/s, the influence of the porosities on the migration of DNAPL is shown in Fig. 13. The porosity affects only the time delay, and does not affect the change in the migration process (i.e., the curves in Fig. 13 are almost the same). The rate of the DNAPL migration and the maximum DNAPL saturation increase with decreasing porosity.

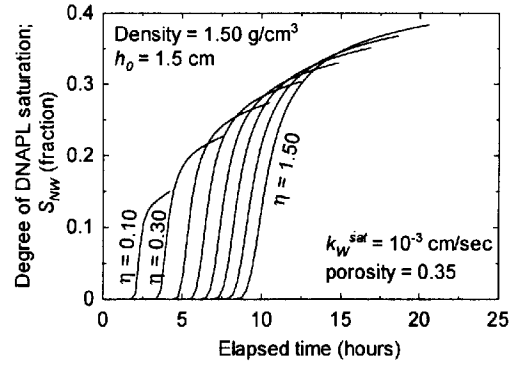


**Fig. 10** Influence of the DNAPL viscosity on the migration process

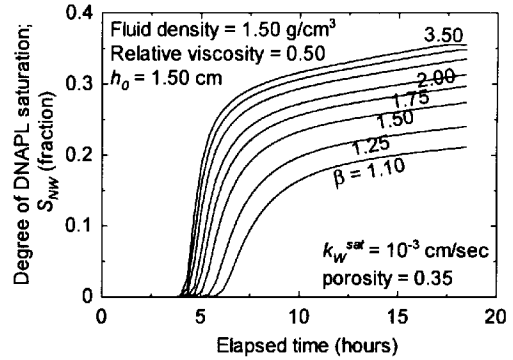


**Fig. 11** Influence of the interfacial tension ( $\beta_{ij}$ ) on the migration process

### 3.2 Comparison

Figure 14 shows the experimental and the numerical results of the column modeling test, in which the left figure shows the results obtained by using the HFE-7100 as the substitute DNAPL, and right one shows the results obtained by the PF-5080. The opened and closed circles with lines indicate the experimental results, and the dotted and broken lines stand for the numerical results. Since PF possesses high viscosity, the migration of PF is slower than the HFE, according to the Darcy's law which is expressed as Eqn.(3). Considering that the elapsed time is 60 minutes in this figure, the experimental results are inconsistent with the numerical results. This inconsistency would be due to the boundary condition. The boundary of the bottom of the column experiment is a permeable boundary for both water and DNAPL, while that of the bottom of the numerical analysis is prescribed as an impermeable boundary for DNAPL. Therefore, there exists a different pressure-balance around the bottom between the experiment and the numerical analysis. In the PF system, the measured saturation is less than the numerical values, and the measured rate of the migration is

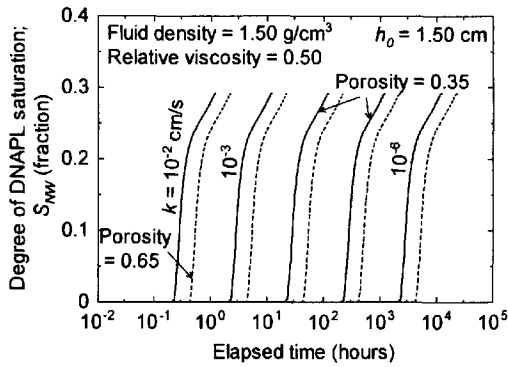


Fig. 12 Influence of the saturated hydraulic conductivity on the migration process

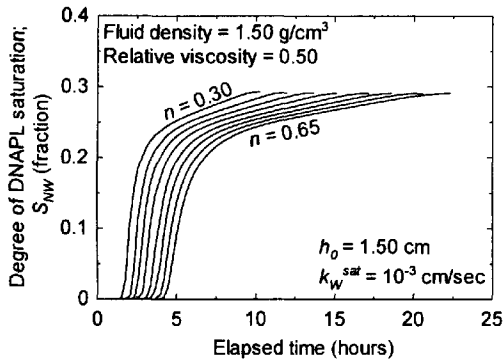


Fig. 13 Influence of the porosity of the porous media on the migration process

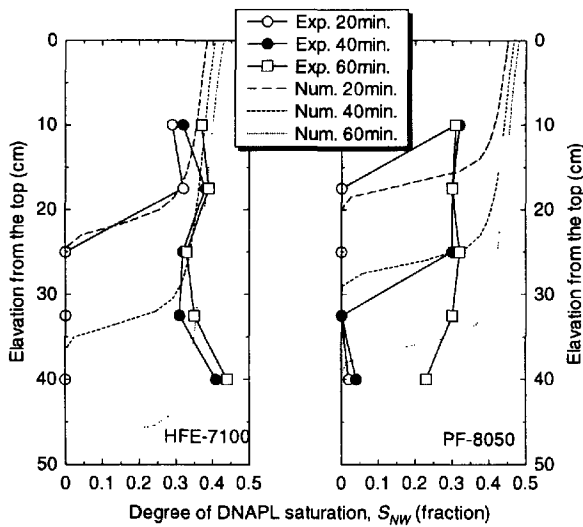


Fig. 14 Comparing the experimental results with the numerical results

also incompatible with the numerical one. It may be said that, however, over all features of the numerical results agree with the experimental ones, though the

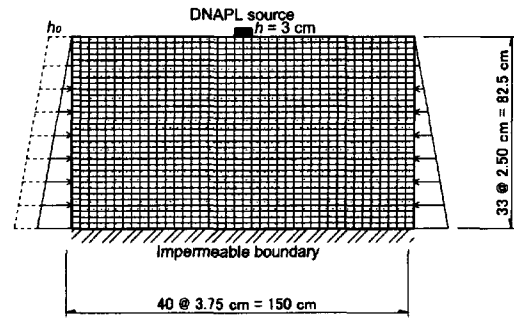


Fig. 15 Boundary condition for the analyses of the homogeneous tank media

boundary condition should be modified.

#### 4. Two-Dimensional Modeling

In actual, since there are only a few information about the subsurface, it is difficult to know the details of geological stratum. Microscopic heterogeneity of geologic media and fluid properties includes complicated problems, and the heterogeneities become serious problems for solving the DNAPL migration. For example, in Fig. 1, if the presence of the clayey soil lens cannot be obtained from some boring data, then it is interpreted that the geological stratum in the contaminated site is homogenous structure. Consequently, the estimation of the migration path way causes an error, and then the efficient design and project for the remediation of toxic chemicals cannot be accomplished. Therefore, the processes of DNAPL migration depending on homogenous and heterogeneous geotechnical structures should be investigated.

##### 4.1 Homogenous porous media

The sand tank, which has  $40 @ 3.75 \text{ cm} = 150 \text{ cm}$  long in width (x-direction) and  $33 @ 2.5 \text{ cm} = 82.5 \text{ cm}$  long in depth (z-direction), saturated with water as a homogenous porous medium is prepared. The sand has the hydraulic conductivity of  $10^{-2} \text{ cm/s}$ , the porosity of 0.35, the VG parameter  $\alpha$  of 0.20, and  $n = 7.00$ . The boundary condition of this analysis is shown in Fig. 15. The top and bottom boundaries of the tank are specified as an impermeable boundary for all fluid phases, and the prescribed water head on both left and right sides are fixed according to the initial conditions allowing water flow through the boundaries. In order to evaluate the influence of the rate of groundwater flow on the direction of DNAPL migration, the top of the



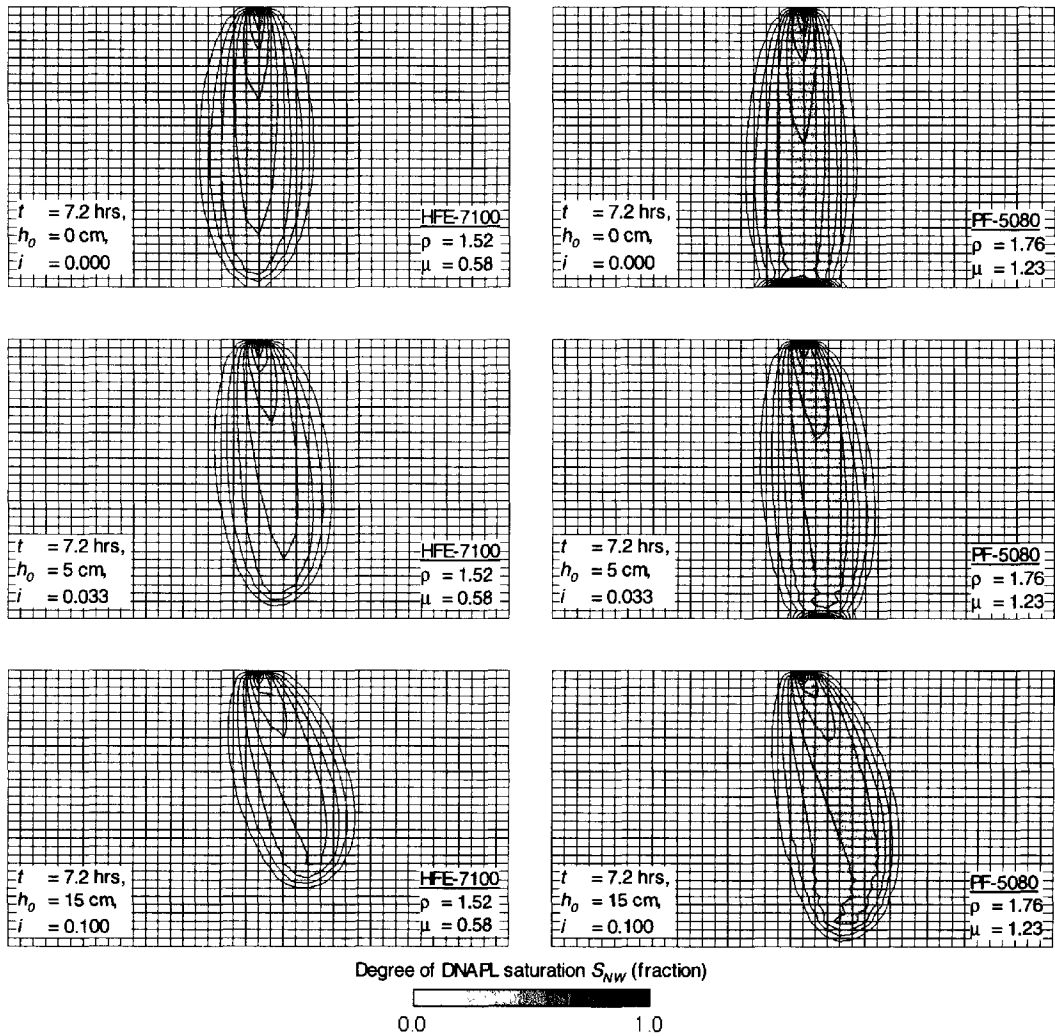


Fig. 16 DNAPLs (HFE-7100 and PF-5080) distribution in the section against the groundwater flow

right boundary is fixed at 0cm head, that is, no external water pressure is applied, while the top of the left boundary is varied from 0cm to 15cm head as applied water pressure heads. DNAPL source is spilled by constant head  $h_\alpha = \rho_\alpha \times 3$  cm at the top of the tank and center of the width. The migration processes of the elapsed time 7.2 hours are investigated by observing the changes in the degree of DNAPL saturation. The results for the tank analysis for estimating the influence of the groundwater flow are shown in Fig. 16. HFE-7100 and PF-5080 (HFE and PF in Fig. 16, respectively) are used for the spilling DNAPL. The applied water heads on the top of left boundary are 0, 5, and 15 cm.

It can be seen from Fig. 16 that, under no groundwater flow condition, the PF with higher density reaches the bottom of the tank and then spreads later-

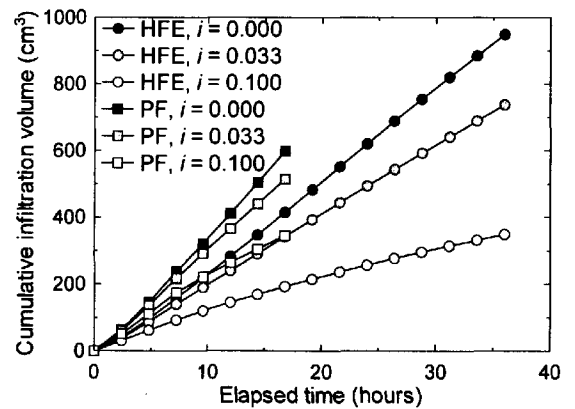
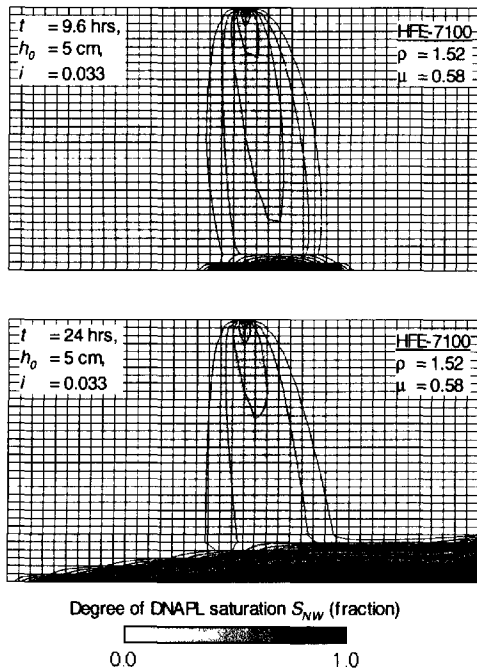


Fig. 17 Relationship between cumulative infiltration volume of DNAPL and elapsed time under the water saturated condition of the homogenous porous system



**Fig. 18** DNAPL distribution for the different elapsed times

ally along the bottom, while the HFE which has lower density than the PF does not reach the bottom. It is interesting to note that even though the PF possesses higher viscosity than the water and HFE, the rate of the downward migration is higher than the HFE. From Fig. 9, the PF migration is inferred to be faster than the HFE. In contrast, considering from Fig. 10, the HFE migration becomes faster than the PF. Thus, in order to predict correctly the rate of a DNAPL migration, coupled effect of the density and viscosity of the fluid should be taken into consideration, and then the migration process should be estimated in terms of the dynamic viscosity of the DNAPL.

It is generally said that the direction of the DNAPL migration is not affected by groundwater flow. From our analytical approaches, however, the directions depend on the rate of groundwater flow. This result would provide useful and efficient parameters to predict the fate of DNAPL contamination and to identify the source point from the boring data regarding the contaminated site. The rate of the groundwater flow is almost constant with respect to time, and furthermore the properties of soil is also stable, in other words, the influence of the groundwater flow and the geotechnical constant on the direction of the DNAPL migration remain to be constant. Therefore, though it would be possible to predict the fate of DNAPL and to iden-

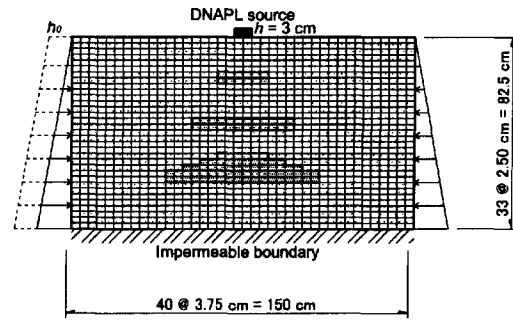


**Fig. 19** Boundary condition for the analyses of the heterogeneous tank media; densely-dotted area means clayey lens

tify the source point of the spilling, more considerations should be given to apply to the real contaminated site, because the real site possesses many heterogeneity conditions.

The relationship between the elapsed time and cumulative infiltration volumes of DNAPL are shown in Fig. 17. Infiltration times are 36 and 13.6 hours for the cases of HFE and PF, respectively. This figure shows the influence of the rate of groundwater flow on the infiltration volume for both cases of HFE and PF. It is found that the infiltration volume increases as the rate of groundwater flow decreases, and, comparing HFE with PF, the larger amount of PF is infiltrated into the tank medium than the HFE.

Assuming that there is an impermeable basement rock at the bottom of a certain subsurface in the contaminated site, the DNAPL spreads laterally along the surface of the basement rock after the DNAPL has reached the basement rock. From Fig. 17, the cumulative infiltration volume of DNAPL continues to increase sequentially, and it is not related to whether or not the DNAPL reaches the bottom. The DNAPL distribution of the tank medium at elapsed times 9.6 and 24 hours is shown in Fig. 18. From this figure, it is seen that the degree of DNAPL saturation above the DNAPL pool at both 9.6 and 24 hours shows a similar distribution. This tendency is an important aspect for the site characterization. If a contaminated condition at the site is surveyed in a shallow region, the contaminated history cannot be obtained because the distribution of toxic chemicals in the site is independent of the passed DNAPL volume after the first imbibition has passed. This theory includes serious problem which has a potentiality to be grown in the near future.

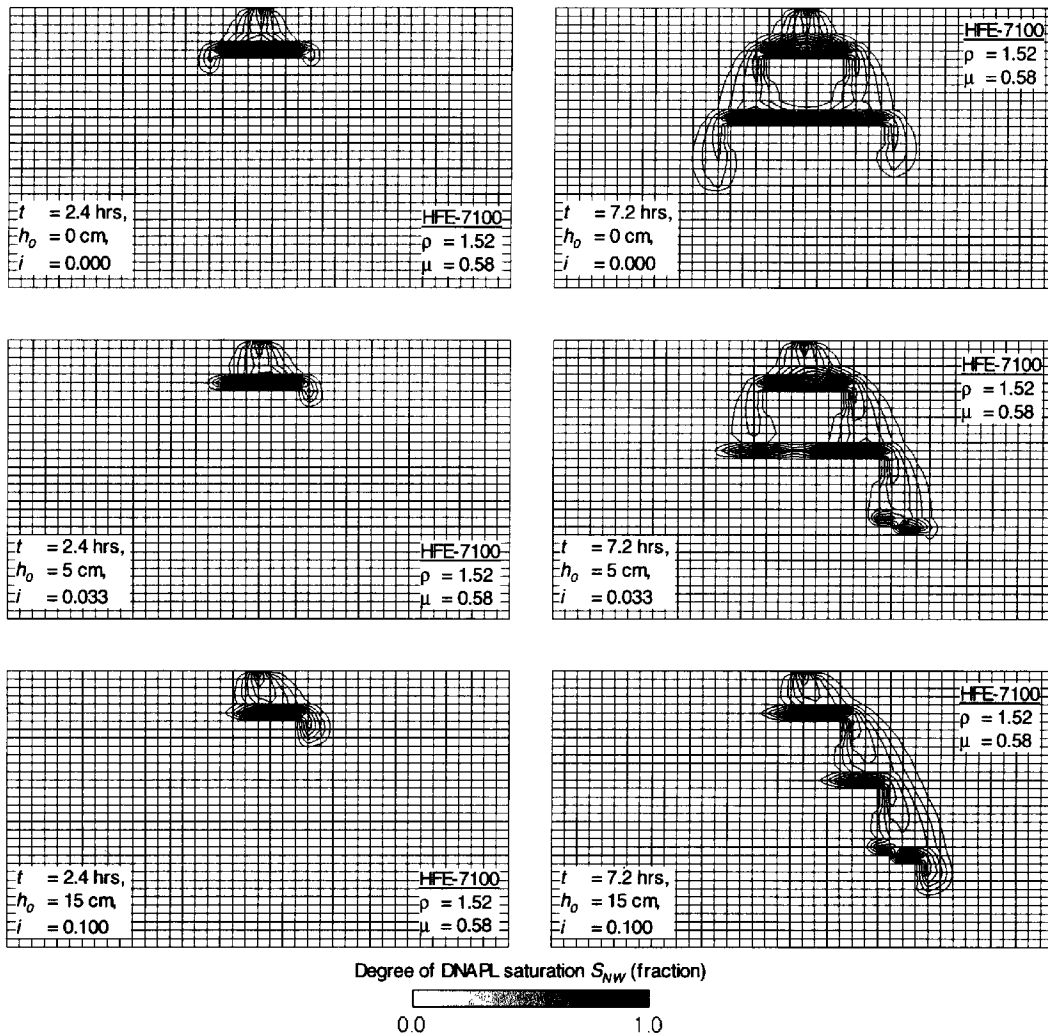


Fig. 20 DNAPL (HFE-7100) distribution in the section against the elapsed time and the groundwater flow

#### 4.2 Heterogeneous porous media

In order to investigate the influence of the heterogeneous porous medium on the DNAPL migration, the numerical analyses are performed by adding three silty lenses to the former homogeneous system. The geometry and boundary condition is shown in Fig.19, in which the densely dotted area indicates silty lenses with hydraulic conductivity of  $k = 10^{-3}$  cm/s, the VG parameter  $\alpha = 0.05$ , and  $n = 6.00$ , and the other regions have  $k = 10^{-2}$  cm/s,  $\alpha = 0.20$ , and  $n = 7.00$ .

Figure 20 shows the HFE-7100 migration processes, in which the diagrams can be divided into three hydraulic gradient cases; 0.000, 0.033, and 0.100 for upper, middle, and lower diagrams, respectively. In the case of no groundwater flow, the degree of DNAPL saturation is expected to distribute symmetrically, with which the calculated results are not consistent. This

would be caused by some numerical errors, and hence it is necessary to modify the numerical conditions. When the groundwater flow exists from left to right, the distribution of DNAPL saturation deforms to the right in a similar tendency as the homogeneous system. When the hydraulic gradient of the groundwater is 0.100, the DNAPL migration from the left side of the first silty lens is not seen. Therefore, if the presence of silty/clayey lens in the contaminated site is overlooked, then it causes the fail to estimate the fate of DNAPL migration.

Figure 21 shows the distribution of the PF-5080 saturation in a homogeneous tank medium in the same system as the HFE migration. Comparing PF and HFE, the distribution of PF widely spreads than the HFE. When the hydraulic gradient is 0.100, a little amount of the PF migration from the left side of the first silty

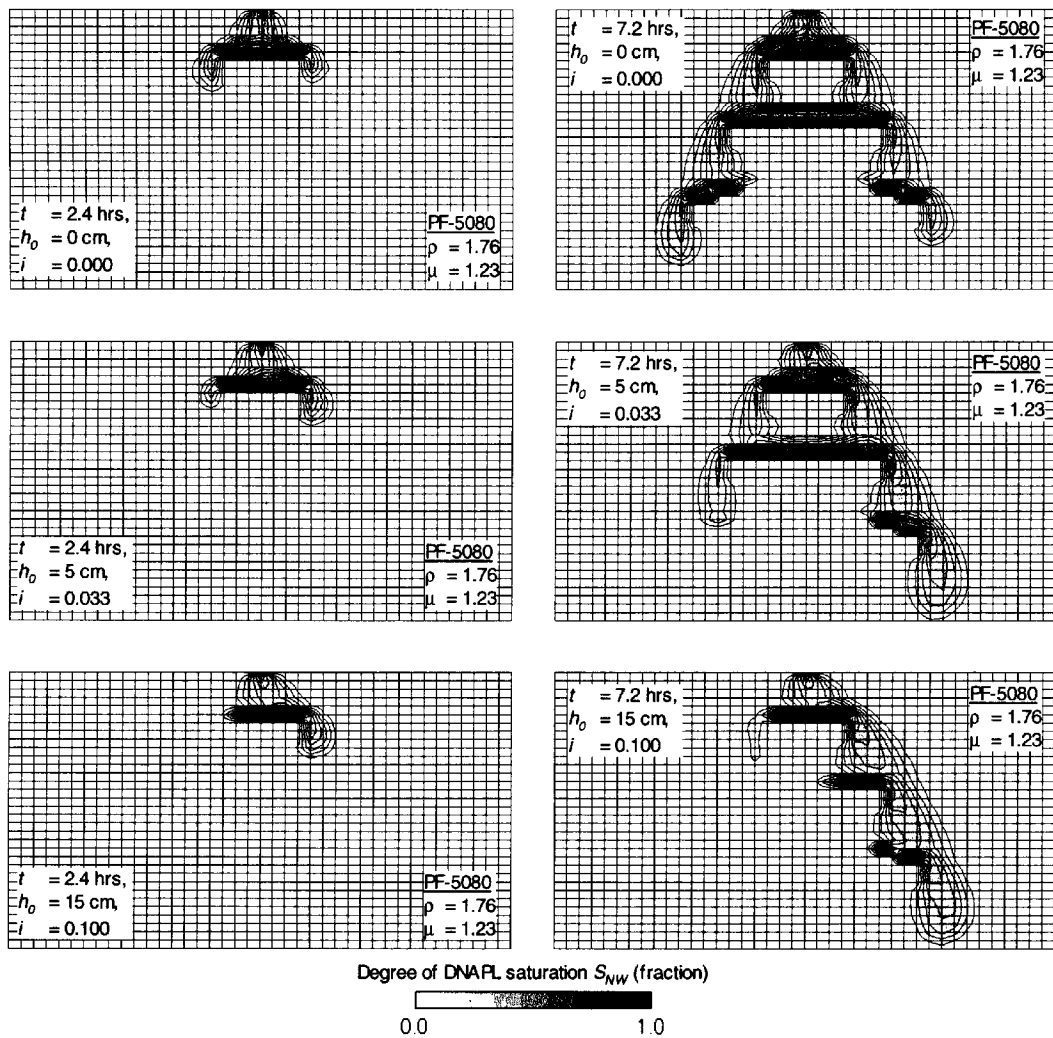


**Fig. 21** DNAPL (PF-5080) distribution in the section against the elapsed time and the groundwater flow

lens can be seen. In the case  $i = 0.033$ , the PF migration from the both side of the first lens can be found. In the case of no groundwater flow, the DNAPL pool forming on the third lens migrates upward and accumulate on the top of the third lens, even though the DNAPL contacts to the second step on the third lens. Also, the DNAPL spreads laterally and migrates downward. As a whole, it is seen that the distribution of the degree of PF saturation takes higher value comparing with the HFE. From this tank analysis, in this condition, the DNAPL cannot invade into the silty/clayey lens having smaller VG parameter  $\alpha$ .

## 5. Conclusions

The DNAPL migration concept under the immiscible liquid-liquid two-phase condition, namely, the

migration concept of DNAPL under the aquifer is presented. This concept, which is clarified by numerical approach, would be expected to be helpful to progress and develop the field of this research and the remediation measures. The main results obtained in this paper are as follows:

- 1) The maximum degree of DNAPL saturation increases with increase in the relative density and relative viscosity and with decrease in the interfacial tension between water and DNAPL.
- 2) The rate of DNAPL migration increases with decreasing relative density and relative viscosity and with increasing interfacial tension between water and DNAPL.
- 3) The decrement of the hydraulic conductivity (i.e., the intrinsic permeability in the porous medium) induces simply the retardation of the migration.

It does not relate to the change in the degree of saturation.

- 4) The rate of DNAPL migration decreases and the degree of DNAPL saturation increases as the porosity of the porous medium increases.
- 5) The DNAPL's vertical downward migration is affected by the direction and the rate of groundwater flow. In the simulation of homogeneous tank modeling, the orientation of the DNAPL migration rotates with respect to the spilling point, depending on the flow rate.
- 6) The infiltration rate of DNAPL with a constant head decreases with increasing rate of the groundwater flow.
- 7) In the case that there exists an impermeable rock/layer at the bottom of the contaminated site, the DNAPL spreads laterally along the surface after the DNAPL reached the impermeable rock/layer, and the cumulative infiltration volume of DNAPL continues to increase without changing the DNAPL distribution above the DNAPL pool.
- 8) In the heterogeneous tank modeling, the DNAPL cannot invade into the silty/clayey lens with higher displacement pressure head, and the DNAPL transports to a mobile region, but the migration is not always downward.

From these results, the migration concept of DNAPL within the aquifer has been clarified. However, the contaminated process of DNAPL is started from the top of the ground surface, and hence the DNAPL passes through the vadose/unsaturated region. In this region, the pore fluids consist of three mobile phases; water, DNAPL, and air. In order to make clear the DNAPL distribution in the subsurface of the contaminated site, immiscible three-phase flow problems should be solved.

The solute transport issue of VOCs and DNAPLs should be taken into the consideration, and then the fate of toxic chemicals should be evaluated from the standpoint of coupled effect of an immiscible multi-phase flow and an advection-dispersion transport. In order to assess the risk on the contaminated site and to characterize the site contamination, the estimation of the entrapped/residual DNAPL, which induces the diffusion of dissolved toxic chemicals from it for a long period, becomes a significant and important issue.

Many numerical models for analyzing the fate and transport of VOCs and DNAPLs have been proposed, but only a few works have been done on the experi-

mental approach for measuring the DNAPL migration properties. This is because an effective experimental method has not yet been developed. Therefore, in order to estimate the efficiency of numerical results and to construct properly a remediation project, the modeling for the experimental approach and the assessment procedure regarding site characterization should be developed.

### Notation

$g$	the gravitational acceleration	[cm/s <sup>2</sup> ]
$h^*$	scaled capillary pressure head	[kPa]
$h_0$	initial water-equivalent head	[cm]
$h_c$	capillary pressure head	[cm]
$h_d$	displacement pressure head (BC parameter)	[cm]
$h_{nw}$	water-equivalent head of non-wetting phase	[cm]
$h_w$	water-equivalent head of wetting phase	[cm]
$K$	intrinsic permeability	[cm <sup>2</sup> ]
$k$	hydraulic conductivity	[cm/s]
$k_{r\alpha}$	relative permeability of $\alpha$ phase	[cm/s]
$m$	VG parameter	[-]
$n$	VG parameter	[-]
$P_a$	pore air pressure	[kPa]
$P_c$	capillary pressure	[kPa]
$P_{nw}$	pore pressure of non-wetting phase	[kPa]
$P_w$	pore pressure of wetting phase	[kPa]
$q_{\alpha i}$	fluid flux of $\alpha$ phase or Darcy velocity	[cm/s]
$Q_\alpha$	source-sink term of $\alpha$ phase	[-]
$r$	radius of curvature	[cm]
$S_\alpha$	degree of $\alpha$ phase saturation	[-]
$S_{je}$	effective $j$ -phase saturation	[fraction]
$S_{jr}$	residual/irreducible $j$ -phase saturation	[fraction]
$v$	real velocity of the fluid	[cm/s]
$z$	elevation from a datum line	[cm]
$\alpha$	VG parameter	[1/cm]
$\epsilon$	conductivity of pore structure	[-]
$\gamma$	conductivity of pore structure	[-]
$\lambda$	pore distribution index (BC parameter)	[-]
$\mu_\alpha$	viscosity of $\alpha$ phase	[mPa · s]
$\phi$	angle of an orientation of solid surface	[degree]
$\Phi$	porosity of a porous media	[-]
$\rho_\alpha$	density of $\alpha$ phase	[g/cm <sup>3</sup> ]
$\rho_w$	density of water	[g/cm <sup>3</sup> ]
$\sigma$	interfacial/surface tension	[mN/m]
$\sigma^*$	interfacial tension of reference fluid pair	[mN/m]
$\sigma_{ij}$	interfacial tension between fluids $i$ and $j$	[mN/m]
$\theta$	contact angle	[degree]

## References

- Bear, J. (1972) : *Dynamics of Fluids in Porous Media*, Dover Publications.
- Brooks, R. H. and Corey, A. T. (1964) : Hydraulic properties of porous media, in *Hydrology Paper no.3*, Colorado State University, Fort Collins, pp. 1–27.
- Dullien, F. A. L. (1992) : *Porous Media: Fluid Transport and Pore Structure*, Academic Press, 2nd edition.
- Helmig, R. (1997) : *Multiphase Flow and Transport Processes in the Subsurface*, Springer.
- Kaluvarachi, J. J. and Parker, J. C. (1989): An efficient finite element method for modeling multiphase flow, Vol. 25, No. 1, pp. 43–54.
- Kinzelbach, W. (1986) : *Ground water Modelling: An Introduction with Sample Programs in BASIC*, Elsevier.
- Lenhard, R. J. and Parker, J. C. (1987a): Measurement and prediction of saturation-pressure relationships in three-phase porous media systems, *J. Contam. Hydrol.*, Vol. 1, pp. 407–424.
- Lenhard, R. J. and Parker, J. C. (1987b): A model for hysteretic constitutive relations governing multiphase flow. 2. permeability-saturation relations, *Water Resour. Res.*, Vol. 23, No. 12, pp. 2197–2206.
- Kamon, M., Endo, K., and Katsumi, T. (2001): Experimental investigation on the properties of DNAPLs migration, *3rd BGA Geoenviron. Engrg. Conf.*, (submitted).
- Parker, J. C. and Lenhard, R. J. (1987): A model for hysteretic constitutive relations governing multiphase flow. 1. saturation-pressure relations, *Water Resour. Res.*, Vol. 23, No. 12, pp. 2187–2196.
- Parker, J. C. (1989): Multiphase flow and transport in porous media, *Reviews of Geophysics*, Vol. 27, No. 3, pp. 311–328.
- Perloff, W. H. and Baron, W. (1976) : *Soil Mechanics: Principles and Applications*, Ronald Press Corporation.
- van Genuchten, M. Th. (1980): A closed-form equation for predicting the hydraulic conductivity of unsaturated soils, *Soil Sci. Soc. Am. J.*, Vol. 44, pp. 892–898.

## DNAPLsの物性と地盤定数が浸透特性に及ぼす影響

嘉門雅史・遠藤和人\*・勝見 武\*\*

\* 京都大学大学院工学研究科

\*\* 立命館大学理工学部

### 要 旨

高密度非水溶性流体相 (DNAPL) の地盤内の浸透特性は相対透水係数 ( $k$ )、飽和度 ( $S$ )、間隙水圧 ( $p$ ) の関係で表すことが可能である。これら3個のパラメーターの関係は  $k$ - $S$ - $p$  relation と呼ばれるもので、水・空気2相流系、すなわち不飽和浸透における関係と同義である。本研究の目的は、非混合性の液液2相流下における  $k$ - $S$ - $p$  relation を明確にしようとするものである。地盤内における液液2相流の概念を明確にし、DNAPL、ならびに地盤特性が  $k$ - $S$ - $p$  relation に及ぼす影響を、二次元有限要素コード MOFAT を利用し解析的に求めた。解析は1次元カラムモデルと2次元土槽モデルを対象として行った。これらの解析結果は浄化手法や DNAPL 浸透の行方を評価する上で有効となる基本的概念を示すものである。

キーワード：DNAPLs,  $k$ - $S$ - $p$  relations, 流体特性, 地盤工学的定数, 地下水流